

Pyridinium-based ionic liquid crystals with terminal fluorinated pyrrolidine

Jingqi Tao^a, Junwen Zhong^a, Peilian Liu^a, Stelck Daniels^c, Zhuo Zeng^{a,b,*}

^a College of Chemistry & Environment, South China Normal University, Guangzhou 510006, China

^b Key Laboratory of Organofluorine Chemistry, Shanghai Institute of Organic Chemistry, Chinese Academy of Sciences, Shanghai 200032, China

^c Department of Chemistry, University of Idaho, Moscow, ID 83844-2343, USA

ARTICLE INFO

Article history:

Received 1 May 2012

Received in revised form 2 July 2012

Accepted 18 July 2012

Available online 25 July 2012

Keywords:

Liquid crystals

Chemical synthesis

Different scanning calorimetry

Fluorinated pyrrolidine

ABSTRACT

A new class pyridinium-based liquid crystals with an extended fluorinated pyrrolidine were synthesized. These compounds show a wide mesophase range and are stable to high temperatures after an introduction of a fluorinated pyrrolidine to the terminal end. Their properties were modified by varying alkyl substituents on the pyridinium ring. The mesophase behavior was affected by altering the configuration of the terminal fluorinated heterocycle. For a comparison, the analogs **5a–5c** with an extended fluorinated azepine were also synthesized. The terminal seven-membered 3,3,4,4,5,5,6,6-octafluoroazepane formed an “L” shape. The twisted L configuration significantly impacted the liquid crystal behavior of **5a–5c**, resulting from steric hindrance. The structures of **3b** were investigated using single crystal X-ray diffraction analysis.

© 2012 Elsevier B.V. All rights reserved.

1. Introduction

Ionic liquid crystals (ILCs), widely used materials, have combined the properties of both ionic liquids and liquid crystals [1]. These self-organizing systems offer great advantages over isotropic systems. The ion conduction was enhanced in the SmA and columnar phases as compared to that in the isotropic phase [2]. The unique properties of ionic liquid crystals have invited a widespread application in display technology and in other areas such as solar cells [3], ion conductors [4,5], and templates for nanoparticles [6,7]. It is well established that the driving force for the formation of ionic LCs are hydrophobic, dipole–dipole, and cation– π interactions, as well as the π – π stacking of the aryl groups [8]. The introduction of a strong electron donating or withdrawing group will change these inter or intramolecular forces. Applying this strategy, one can modify the ILCs physical and crystal properties [9].

The introduction of a fluorine atom or fluorinated group into liquid crystals systems will change the formation of these materials, which may elicit interest in display and non-display applications [10]. Compared to non-fluorinated liquid crystals, these liquid crystals with fluorinated substituents have some advantages, such as, broader nematic phase ranges, lower melting points, high dielectric anisotropy, and good voltage ratios [11].

Some fluorinated liquid crystals (FLCs) of fused ring systems for TFT-LCD are currently commercially available.

The merger of ILCs and FLCs yields fluorinated ionic liquid crystals (FILCs). In the recent years, the number of articles reporting ILCs has risen dramatically [12–23]. Some of these reported ILCs are shown in Scheme 1. However, fluorinated ionic liquid crystals (FILCs) are not widely reported in spite of their potential unique applications.

The 1,2,4-oxadiazolylpyridinium salts with terminal highly fluorinated alkyl chain were reported by Lo Celso [24]. Recently, Li [25] has synthesized fluorinated imidazolium-based dicationic ionic liquid crystals using fluoro-substituents as linking bridges. By introducing two perfluoroalkyl chains at the 2 and 6 positions of the pyridine ring, Rocaboy [26] obtained SmB Phase FILCs. For the lateral fluorinated ILCs, the mesophase behavior is affected by the position of the fluorine atom due to the influence of intermolecular forces [27].

The installation of a fluorinated heterocycle into ILCs has rarely been reported. The reported synthetic routine for these heterocycles often use HF, or F₂ as a fluorinating reagent or complicated building blocks. These reagents make the purification difficult and expensive. It is possible that fluorobenzene in the ILCs can be replaced by the fluorinated heterocycles, inviting a study of structure–properties are their relationship in FILCs. New FILCs bearing fluorinated heterocycles will prove highly valuable because these new FILCs may have advantageous applications. The factors affecting the properties of ionic liquid crystals include (1) the nature of the terminal fluorinated heterocycles, (2) the configuration of the fluorinated heterocycles, and (3) the substituent group on the cations. Here we are reporting the preparation and physical properties of a new series of FILCs

* Corresponding author at: College of Chemistry & Environment, South China Normal University, Guangzhou 510006, China. Fax: +86 20 3931 0287.

E-mail address: zhuoz@sncnu.edu.cn (Z. Zeng).

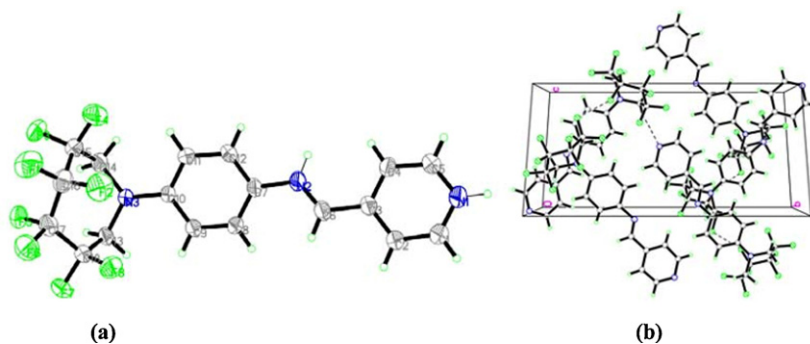


Fig. 1. (a) Displacement ellipsoid plot of **3b**. Hydrogen atoms are included but unlabelled for clarity. (b) Packing diagram of the extended structure of **3b** viewed down the *a*-axis. Dashed lines indicate hydrogen bonding (for **3b** CCDC reference number 822734).

Table 1
Transition temperatures (°C) of new compounds.

Compound	R	Phase behavior						
4a	C ₁₄ H ₂₉	Cr	86.7	M	155.5			Iso ^d
4b	C ₁₆ H ₃₃	Cr	89.9	M	158.8	SmA	174.9	Iso ^d
4c	C ₁₈ H ₃₇	Cr	94.7	M	154.4	SmA	193.2	Iso ^d
5a	C ₁₄ H ₂₉	Cr	79.6					Iso
5b	C ₁₆ H ₃₃	Cr	80.0					Iso
5c	C ₁₈ H ₃₇	Cr	83.9					Iso

Cr = crystalline state; M = mesophase M; SmA = smectic A phase; Iso = isotropic liquid state; Δ = transition temperature detect by POM; d = decompose.

4a–4c and **5a–5c** were investigated by differential scan calorimetry (DSC), thermal gravimetric analysis (TGA) and polarizing optical microscopy (POM). The transition temperatures for all the new fluorinated ionic liquid salts are shown in Table 1.

Compounds **4a–4c**, which bear the 3,3,4,4-tetrafluoropyrrolidine as terminal fluoro-substituent, show good liquid crystal properties. Compound **4a** had two endothermic peaks at 86.4 °C and 155.5 °C in the DSC figure. Longer alkyl n-C₁₆H₃₃ or n-C₁₈H₃₇ substituents on the pyridine increased the transition temperature of the melting point and the clearing point. **4b** showed a large enthalpy transition followed by two transitions with smaller enthalpy changes indicating the presence of two mesophases. These peaks in the heating cycle were at 89.9 °C, 158.8 °C and 174.9 °C. Compound **4c** also showed three endothermic peaks in the heating cycle, at 94.7 °C, 154.4 °C and 193.2 °C (Fig. 2). Investigation of the optical textures by polarizing microscopy revealed that the transition at 89.9 °C is the melting point of **4b**, and the melting phase is anisotropic indicating the presence of a mesophase, observed as grainy texture (Fig. 3). Such texture has been reported by Ster [29], Balamurugan and Ravikrishnan

[30–32], and from henceforth it will be referred to as M. The mesophase M appears in all the ionic liquid crystal compounds in this paper. The second peak in the thermogram is at 158.8 °C corresponding to LCI–LCII transition peak, a fan-shape texture (Fig. 3) was observed. The peak at 174.9 °C is the clearing point. Thermal stabilities ranging from 205 °C to 233 °C for **4a–4c** were determined by thermal gravimetric analysis (TGA). Data shows that the decomposition temperatures were higher than the clearing point for these compounds. **4a**, **4b**, and **4c** had a *T_d* at 231.5 °C, 233.4 °C, and 205.4 °C respectively.

Surprisingly, the substitution of the tetrafluoropyrrolidine moiety with octafluoroazepane resulted in the loss of liquid crystal properties. The result was verified by DSC as there was only one endothermic peak in the heating cycle (see supporting information).

All the POM pictures were taken at different temperatures on the heating cycle according to DSC. Observations were made under 50× magnification. The initial heating rate of 10 °C min⁻¹ was slowed to 2 °C min⁻¹ when the temperature was nearing the clearing point. POM typical textures of thermotropic liquid crystal

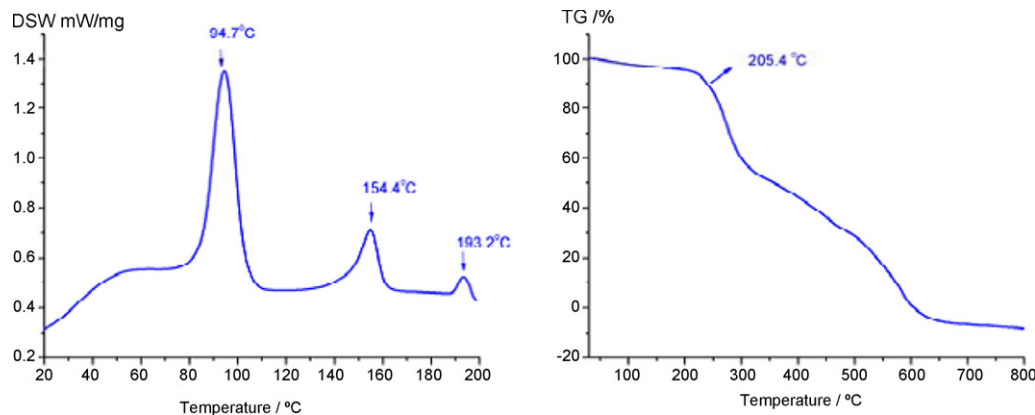


Fig. 2. The DSC (a) and TG (b) trace of **4c**.

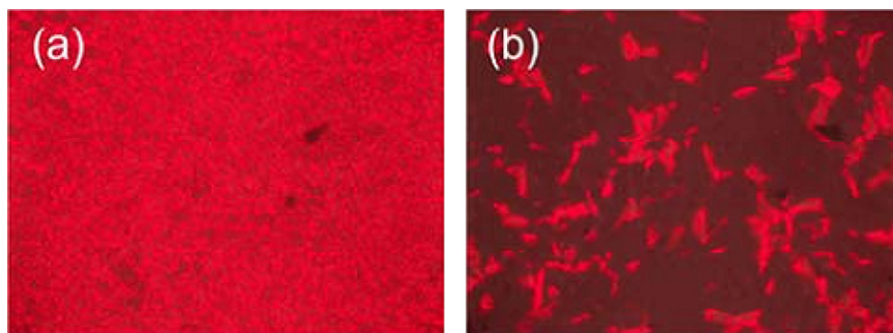


Fig. 3. POM texture for compound **4b** at (a) 152 °C and (b) 162 °C.

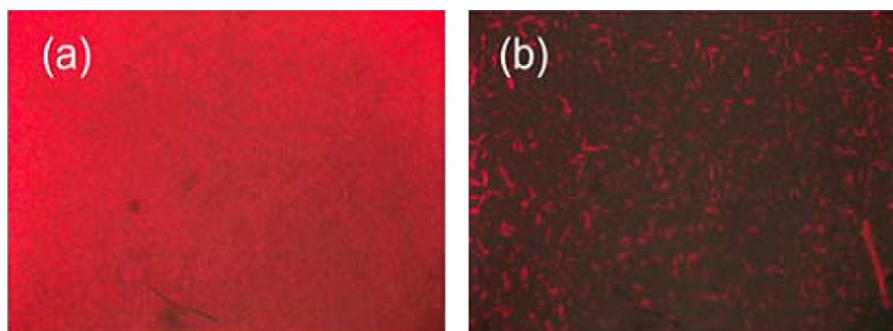


Fig. 4. POM texture for compound **4c** at (a) 131 °C and (b) 177 °C.

phase were observed for compound **4a–4c**. The typical texture change is shown in the following figures for compound **4b**, **4c** (Figs. 3 and 4).

2.3. Discussion

2.3.1. Evaluation of the influence of the alkyl chain

For compound **4a–4c**, the phase transition temperature increases with an increase of the alkyl substituent length. An increase of the chain length also enhances the SmA phase and decreases the mesophase M range, e.g., **4b** with [C₁₆H₃₃] as chain, Cr 89.9 M 158.8 SmA 174.9, **4c** with [C₁₈H₃₇] as chain, Cr 94.7 M 154.4 SmA 193.2.

2.3.2. Influence of the terminal fluorinated heterocycle

The introduction of a polyfluoroalkyl group increases the van der Waals interactions which contribute to the liquid crystal properties of the ionic liquid crystal. The fluorinated heterocycle containing the CF₂ groups tend to have extensive intermolecular or intramolecular hydrogen bonding and exhibit C–F...F weak interaction in the molecules. Compounds **5a–5c** having the terminal seven membered fluorinated azepine do not exhibit liquid crystal properties. Comparatively, compounds **4a–4c**, having a five membered fluorinated pyrrolidine, increase the mesophase range remarkably. The results indicate that the configuration of compounds impact the liquid crystal properties significantly. This is the first study on the relationship between the terminal fluorinated heterocycle configuration and their effects on liquid crystal properties. The twisted configuration of seven membered fluorinated azepine diminishes the liquid crystal properties dramatically. Meanwhile, the planar configuration of five membered fluorinated pyrrolidine increases the mesophase range significantly and exhibits good liquid crystal characteristics.

3. Conclusion

We have synthesized and characterized novel ionic liquid crystals containing fluorinated pyrrolidine as the terminal

heterocycle. The salts displayed good liquid crystals properties. The properties of these ionic liquid crystals can be adjusted by varying the terminal substituent. They show a wide mesophase range and are mesophase stable to high temperature. The salts, which bear the seven membered fluorinated azepine as terminal heterocycle, do not show liquid crystal properties. The twisted configuration of a fluorinated azepine reduced the liquid crystal properties drastically. It was also found that terminal fluorinated heterocycle configurations have a great impact on liquid crystal properties. Further research should provide broad insight into the development of the novel liquid crystals.

4. Experimental

4.1. General considerations

All the reagents were analytical grade, purchased from commercial sources and used as received. ¹H, ¹⁹F and ¹³C NMR spectra were recorded on a 400 MHz nuclear magnetic resonance spectrometer operating at 400, 376 and 175 MHz respectively. Chemical shifts were reported relative to Me₄Si for ¹H, and ¹³C, and CCl₃F for ¹⁹F. The solvent was CDCl₃ unless otherwise specified. The DSC was recorded on a differential scanning calorimeter at a scan rate of 2 °C min⁻¹. Optical micrographs were observed with a polarizing optical microscope (POM) (Nikon LINKAM-THMSE600); Elemental analyses were performed on an EXETER CE-440 Elemental Analyzer.

4.2. General procedure for the preparation of trifluoromethanesulfonic acid polyfluoroalkyldiyl ester **1a–1b**

2,2,3,3-Tetrafluoro-1,4-butanediol (1 mmol), 2,2,3,3,4,4,5,5-octafluoro-1,6-hexanediol, **1b** (1 mmol), pyridine (2.5 mmol) and dichloromethylene (20 mL) were stirred at room temperature. After 20 min, trifluoromethanesulfonic anhydride (2.5 mmol) in 10 mL dichloromethylene was slowly added over 1 h. The mixture was stirred for 12 h, then washed with water (3 × 30 mL), and dried over anhydrous sodium sulfate. The solvent was removed

under vacuum to give trifluoromethanesulfonic acid polyfluoroalkylidyl ester [33], **1a–1b**.

4.2.1. 4-(3,3,4,4-Tetrafluoropyrrolidin-1-yl)benzenamine (**2a**)

Trifluoromethanesulfonic acid 2,2,3,3-tetrafluoro-1,4-butane-dilyl ester, **1a** (2 mmol), p-phenylenediamine (3 mmol), and Et₃N (5 mmol) in 25 mL ethanol were placed in a round-bottomed flask fitted with a reflux condenser, and heated at reflux for 30 h. After cooling, the organic solvent was removed under reduced pressure, to the residue was added 50 mL dichloromethane then washed with water (3 × 20 mL). The organic layer was dried over anhydrous Na₂SO₄. After the solvent was removed, the crude product was purified by column chromatography. The product was isolated using dichloromethane–petroleum ether (1:1) as eluent to give **2a**.

2a: Yield, 76%, white solid. ¹H NMR (400 MHz, CDCl₃, TMS) δ: 6.69 (d, J = 8.7 Hz, 2H), 6.42 (d, J = 8.7 Hz, 2H), 3.73 (m, 4H), 3.66–2.54 (br, 2H) ppm. ¹⁹F NMR (376 MHz, CDCl₃) δ: –123.04 to –123.39 (m, 4F) ppm. MS (ESI) *m/z*: 235.53(M+H⁺). Anal. Calcd. for [C₁₀H₁₀F₄N₂]: C, 51.29; H, 4.30; N, 11.96. Found: C, 50.77; H, 4.48; N, 11.79.

4.2.2. 4-(3,3,4,4,5,5,6,6-Octafluoroazepan-1-yl)benzenamine (**2b**)

Trifluoromethanesulfonic acid 2,2,3,3,4,4,5,5-octafluoro-1,6-hexanedilyl ester p-phenylenediamine (3 mmol), and Et₃N (5 mmol) in 25 mL ethanol were placed in a round-bottomed flask fitted with a reflux condenser, and heated at reflux for 30 h. After cooling, the organic solvent was removed under reduced pressure. 50 mL of dichloromethane was added to the residue and then washed with water (3 × 20 mL). The organic layer was dried over anhydrous Na₂SO₄. After the solvent was removed, the crude product was purified by silica gel column chromatography [SiO₂, CH₂Cl₂/PE 3:5, v/v] to give a white solid.

2b: Yield, 56%. ¹H NMR (400 MHz, CDCl₃) δ: 6.81 (d, J = 8.5 Hz, 2H), 6.64 (d, J = 8.6 Hz, 2H), 3.88 (t, J = 12.7 Hz, 4H), 2.62 (br, 2H). ¹⁹F NMR (376 MHz, CDCl₃) δ: –113.30 (s, 4F), –128.40 (s, 4F) ppm. MS (ESI) *m/z*: 335.58 (M+H⁺). Anal. Calcd. for [C₁₂H₁₀F₈N₂]: C, 43.13; H, 3.02; N, 8.38. Found: C, 42.98; H, 3.38; N, 8.07.

4.2.3. 4-(3,3,4,4-Tetrafluoropyrrolidin-1-yl)-N-((pyridin-4-yl)methylene)benzenamine (**3a**)

To a solution of **2a** (0.2009 g, 0.85 mmol) and pyridine-4-carbaldehyde (0.1364 g, 1.275 mmol) in 25 mL dichloromethane, was added anhydrous MgSO₄ (16 mmol, 1.636 g), and stirred overnight at room temperature. The inorganic salt was filtered off. To the residue was added 50 mL PE and filtered to give yellow solid.

3a: Yield, 96.54%. ¹H NMR (400 MHz, CDCl₃) δ: 8.72 (d, J = 4.8 Hz, 2H), 8.47 (s, 1H), 7.72 (d, J = 4.7 Hz, 2H), 7.33 (d, J = 7.5 Hz, 2H), 6.57 (d, J = 8.5 Hz, 2H), 3.86 (m, 4H). ¹⁹F NMR (376 MHz, CDCl₃) δ: –123.04 to –123.39 (m, 4F) ppm. MS (ESI) *m/z*: 324.65(M⁺). Anal. Calcd. for [C₁₆H₁₃F₄N₃·0.5H₂O]: C, 57.83; H, 4.25; N, 12.65. Found: C, 58.00; H, 4.27; N, 12.79.

4.2.4. 4-(3,3,4,4,5,5,6,6-Octafluoroazepan-1-yl)-N-((pyridin-4-yl)methylene)benzenamine (**3b**)

To a solution of **2b** (0.1671 g, 0.5 mmol) and pyridine-4-carbaldehyde (0.0802 g, 0.75 mmol) in 25 mL dichloromethane, was added anhydrous MgSO₄ (8 mmol, 0.9844 g), and stirred overnight at room temperature. The inorganic salt was removed by filtration. To the residue was added 50 mL PE and filtered to give yellow solid.

3b: Yield 94.98%. ¹H NMR (400 MHz, CDCl₃) δ: 8.71 (d, J = 4.3 Hz, 2H), 8.44 (s, 1H), 7.71 (d, J = 5.1 Hz, 2H), 7.27 (d, J = 8.7 Hz, 2H), 6.96 (d, J = 8.8 Hz, 2H), 4.08 (t, J = 12.2 Hz, 4H). ¹⁹F NMR (376 MHz, CDCl₃) δ: –112.58 (s, 4F), –128.56 (s, 4F) ppm. MS (ESI) *m/z*: 424.57(M⁺). Anal. Calcd. for [C₁₈H₁₃F₈N₃·0.5H₂O]: C, 50.01; H, 3.26; N, 9.72. Found: C, 49.87; H, 3.24; N, 9.51.

4.3. General procedure for the preparation of N-alkyl-4'-substituted-stilbazolium salts **4a–4c**

4-(3,3,4,4-tetrafluoropyrrolidin-1-yl)-N-((pyridin-4-yl)methylene)benzenamine (0.15 mmol, 0.0468 g) and n-alkyl bromide (0.25 mmol) were heated in 5 mL acetonitrile for 12 h under reflux. After cooling to room temperature, the solvent was removed under vacuum to give crude product, which was recrystallized from ethanol–P.E. (1:5) to yield the compounds **4a–4c** in modern yield.

4a: Yield: 43%. ¹H NMR (400 MHz, CDCl₃) δ: 9.26 (d, J = 6.5 Hz, 2H), 8.85 (s, 1H), 8.48 (d, J = 6.5 Hz, 2H), 7.50 (d, J = 8.9 Hz, 2H), 6.55 (d, J = 9.0 Hz, 2H), 4.89 (t, J = 7.4 Hz, 2H), 3.86 (m, 4H), 2.04–1.93 (m, 2H), 1.31–1.10 (m, 22H), 0.83 (t, J = 6.8 Hz, 3H). ¹⁹F NMR (376 MHz, CDCl₃) δ: –123.16 to –123.23 (m, 4F) ppm. MS (ESI) *m/z*: 520.69 [M⁺]. HR-MS (EI) Calcd. for [C₃₀H₄₂BrF₄N₃–Br]⁺: 520.3302 Found, 520.3309.

4b: Yield: 57.6%. ¹H NMR (400 MHz, CDCl₃) δ: 9.22 (d, J = 6.4 Hz, 2H), 8.89 (s, 1H), 8.50 (d, J = 6.4 Hz, 2H), 7.52 (d, J = 8.8 Hz, 2H), 6.56 (d, J = 8.8 Hz, 2H), 4.87 (t, J = 7.2 Hz, 2H), 3.86 (m, 4H), 2.00 (m, 2H), 1.21 (m, 26H), 0.85 (t, J = 6.8 Hz, 3H). ¹⁹F NMR (376 MHz, CDCl₃) δ: –123.13 to –123.21 (m, 4F) ppm. MS (ESI) *m/z*: 548.36 [M⁺]. Anal. Calcd. for [C₃₂H₄₆BrF₄N₃·2H₂O]: C, 57.83; H, 7.58; N, 6.32. Found: C, 57.74; H, 7.07; N, 6.51.

4c: Yield: 48%. ¹H NMR (400 MHz, CDCl₃) δ: 9.25 (d, J = 6.5 Hz, 2H), 8.85 (s, 1H), 8.48 (d, J = 6.4 Hz, 2H), 7.51 (d, J = 8.9 Hz, 2H), 6.56 (d, J = 8.9 Hz, 2H), 4.89 (t, J = 7.2 Hz, 2H), 3.95–3.74 (m, 4H), 2.21–1.81 (m, 2H), 1.20 (m, 29H), 0.84 (t, J = 6.9 Hz, 3H). ¹⁹F NMR (376 MHz, CDCl₃) δ: –123.17 to –123.24 (m, 4F) ppm. MS (ESI) *m/z*: 576.83 [M⁺]. Anal. Calcd. for [C₃₄H₅₀BrF₄N₃·1.5H₂O]: C, 59.73; H, 7.81; N, 6.15. Found: C, 59.88; H, 7.72; N, 5.8.

4.4. General procedure for the preparation of N-alkyl-4'-substituted-stilbazolium salts **5a–5c**

4-(3,3,4,4,5,5,6,6-Octafluoroazepan-1-yl)-N-((pyridin-4-yl)methylene)benzenamine (0.15 mmol, 0.0635 g) and n-alkyl bromide (0.25 mmol) were heated in 10 mL acetonitrile for 12 h under reflux. After cooling to room temperature, the solvent was removed under vacuum to give crude product, which was recrystallized from ethanol–P.E. (1:10) to give the compounds **5a–5c** in modern yield.

5a: Yield: 50%. ¹H NMR (400 MHz, CDCl₃) δ: 9.11 (d, J = 6.5 Hz, 2H), 8.89 (s, 1H), 8.52 (d, J = 6.5 Hz, 2H), 7.49 (d, J = 9.0 Hz, 2H), 6.99 (d, J = 9.1 Hz, 2H), 4.80 (t, J = 7.3 Hz, 2H), 4.15 (t, J = 12.1 Hz, 4H), 2.07–1.97 (m, 2H), 1.20 (m, 22H), 0.84 (t, J = 6.8 Hz, 3H). ¹⁹F NMR (376 MHz, CDCl₃) δ: –112.34 (s, 4F), –128.50 (s, 4F). MS (ESI) *m/z*: 620.71 [M⁺]. Anal. Calcd. for [C₃₂H₄₂BrF₈N₃·2H₂O]: C, 52.18; H, 6.29; N, 5.70. Found: C, 52.26; H, 6.18; N, 5.89.

5b: Yield: 51%. ¹H NMR (400 MHz, CDCl₃) δ: 9.16 (d, J = 6.5 Hz, 2H), 8.93 (s, 1H), 8.53 (d, J = 6.5 Hz, 2H), 7.49 (d, J = 9.0 Hz, 2H), 6.98 (d, J = 9.1 Hz, 2H), 4.82 (t, J = 7.3 Hz, 2H), 4.14 (t, J = 12.1 Hz, 4H), 2.00 (m, 2H), 1.21 (m, 26H), 0.84 (t, J = 6.8 Hz, 3H). ¹⁹F NMR (376 MHz, CDCl₃) δ: –112.36 (s, 4F), –128.51 (s, 4F). MS (ESI) *m/z*: 648.78 [M⁺]. Anal. Calcd. for [C₃₄H₄₆BrF₈N₃·1.5H₂O]: C, 54.04; H, 6.54; N, 5.56. Found: C, 54.50; H, 6.67; N, 5.39.

5c: Yield: 53%. ¹H NMR (400 MHz, CDCl₃) δ: 8.95 (d, J = 6.6 Hz, 2H), 8.81 (s, 1H), 8.48 (d, J = 6.6 Hz, 2H), 7.47 (d, J = 9.0 Hz, 2H), 6.97 (d, J = 9.1 Hz, 2H), 4.71 (t, J = 7.4 Hz, 2H), 4.11 (t, J = 11.9 Hz, 4H), 2.05–1.96 (m, 2H), 1.18 (m, 30H), 0.81 (t, J = 6.8 Hz, 3H). ¹⁹F NMR (376 MHz, CDCl₃) δ: –112.37 (s, 4F), –128.53 (s, 4F). MS (ESI) *m/z*: 676.80 [M⁺]. Anal. Calcd. for [C₃₆H₅₀BrF₈N₃·1.5H₂O]: C, 55.17; H, 6.82; N, 5.36. Found: C, 55.24; H, 7.59; N, 5.24.

Supporting information

Representative DSC and TGA scans for new salts **4a**, **4b**, **5a**, **5b**, and **5c**. Polarized Optical Microscopy data. Crystallographic Data

and Structure Refinement Parameters of compound **3b** (CCDC reference number 822734).

Acknowledgments

The authors gratefully acknowledge the support of Department of Science and Technology, Guangdong Province. Grant number: 2010A020507001-76, 5300410, FIPL-05-003. The Scientific Research Foundation for the Returned Overseas Chinese Scholars, State Education Ministry.

Appendix A. Supplementary data

Supplementary data associated with this article can be found, in the online version, at <http://dx.doi.org/10.1016/j.jfluchem.2012.07.009>.

References

- [1] P.H.J. Kouwer, T.M. Swager, *Journal of the American Chemical Society* 129 (2007) 14042–14052.
- [2] H. Shimura, M. Yoshio, K. Hoshino, T. Mukai, H. Ohno, T. Kato, *Journal of the American Chemical Society* 130 (2008) 1759–1765.
- [3] N. Yamanaka, R. Kawano, W. Kubo, T. Kitamura, Y. Wada, M. Watanabe, S. Yanagida, *Chemical Communications* (2005) 740–742.
- [4] N. Yamanaka, R. Kawano, W. Kubo, N. Masaki, T. Kitamura, Y. Wada, M. Watanabe, S. Yanagida, *Journal of Physical Chemistry B* 111 (2007) 4763–4769.
- [5] S. Yazaki, M. Funahashi, J. Kagimoto, H. Ohno, T. Kato, *Journal of the American Chemical Society* 132 (2010) 7702–7708.
- [6] W. Dobbs, J.M. Suisse, L. Douce, R. Welter, *Angewandte Chemie International Edition* 45 (2006) 4179–4182.
- [7] A. Taubert, *Angewandte Chemie International Edition* 43 (2004) 5380–5382.
- [8] B. Ringstrand, H. Monobe, P. Kaszynski, *Journal of Materials Chemistry* 19 (2009) 4805–4812.
- [9] K. Binnemans, *Chemical Reviews* 105 (2005) 4148–4204.
- [10] M. Hird, *Chemical Society Reviews* 36 (2007) 2070–2095.
- [11] D. Pauluth, K. Tarumi, *Journal of Materials Chemistry* 14 (2004) 1219–1227.
- [12] J.M. Suisse, S. Bellemin-Lapponnaz, L. Douce, A. Maise-François, R. Welter, *Tetrahedron Letters* 46 (2005) 4303–4305.
- [13] S.K. Pal, S. Kumar, *Tetrahedron Letters* 47 (2006) 8993–8997.
- [14] D. Ster, U. Baumeister, J.L. Chao, C. Tschierske, G. Israel, *Journal of Materials Chemistry* 17 (2007) 3393–3400.
- [15] K. Lava, K. Binnemans, T. Cardinaels, *Journal of Physical Chemistry B* 113 (2009) 9506–9511.
- [16] K. Ohta, T. Sugiyama, T. Nogami, *Journal of Materials Chemistry* 10 (2000) 613–616.
- [17] X. Wang, F.W. Heinemann, M. Yang, B.U. Melcher, M. Fekete, A.-V. Mudring, P. Wasserscheid, K. Meyer, *Chemical Communications* (2009) 7405–7407.
- [18] K. Goossens, K. Lava, P. Nockemann, K. Van Hecke, L. Van Meervelt, K. Driesen, C. Görrler-Walrand, K. Binnemans, T. Cardinaels, *Chemical Engineering Journal* 15 (2009) 656–674.
- [19] J.H. Olivier, F. Camerel, G. Ulrich, J. Barberá, R. Ziessel, *Chemical Engineering Journal* 16 (2010) 7134–7142.
- [20] K. Goossens, P. Nockemann, K. Driesen, B. Goderis, C. Görrler-Walrand, K. Van Hecke, L. Van Meervelt, E. Pouzet, K. Binnemans, T. Cardinaels, *Chemistry of Materials* 20 (2008) 157–168.
- [21] D. Haristoy, D. Tsiourvas, *Chemistry of Materials* 15 (2003) 2079–2083.
- [22] J. Yang, Q. Zhang, L. Zhu, S. Zhang, J. Li, X. Zhang, Y. Deng, *Chemistry of Materials* 19 (2007) 2544–2550.
- [23] M. Marcos, M.B. Ros, J.L. Serrano, M.A. Esteruelas, E. Sola, L.A. Oro, J. Barbera, *Chemistry of Materials* 2 (1990) 748–758.
- [24] F. Lo Celso, I. Pibiri, A. Triolo, R. Triolo, A. Pace, S. Buscemi, N. Vivona, *Journal of Materials Chemistry* 17 (2007) 1201–1208.
- [25] X. Li, D.W. Bruce, J.M. Shreeve, *Journal of Materials Chemistry* 19 (2009) 8232–8238.
- [26] C. Rocaboy, F. Hampel, J.A. Gladysz, *Journal of Organic Chemistry* 67 (2002) 6863–6870.
- [27] D.W. Bruce, S.A. Hudson, *Journal of Materials Chemistry* 4 (1994) 479–486.
- [28] Z. Zeng, B.S. Phillips, J.C. Xiao, J.M. Shreeve, *Chemistry of Materials* 20 (2008) 2719–2726.
- [29] D. Ster, U. Baumeister, J. Lorenzo Chao, C. Tschierske, G. Israel, *Journal of Materials Chemistry* 17 (2007) 3393–3400.
- [30] V. Padmini Tamilenth, *International Journal of Chemical Research* 1 (2010) 35–40.
- [31] S. Balamurugan, P. Kannan, *Journal of Molecular Structure* 934 (2009) 44–52.
- [32] A. Ravikrishnan, P. Sudhakara, P. Kannan, *Polymer Degradation and Stability* 93 (2008) 1564–1570.
- [33] Z. Zeng, J.M. Shreeve, *Journal of Fluorine Chemistry* 130 (2009) 727–732.